






Sparse Array Design via Integer Linear Programming

Yangjingzhi Zhuang , *Student Member, IEEE*, Xuejing Zhang , *Member, IEEE*,
Zishu He , *Senior Member, IEEE*, Maria Sabrina Greco , *Fellow, IEEE*, and Fulvio Gini , *Fellow, IEEE*

Abstract—In this paper, a design framework based on integer linear programming is proposed for optimizing sparse array structures. We resort to binary vectors to formulate the design problem for non-redundant arrays (NRA) and minimum-redundant arrays (MRA). The flexibility of the proposed framework allows for dynamic adjustment of constraints to meet various applicative requirements, e.g., to achieve desired array apertures and mitigate mutual coupling effects. The proposed framework is also extended to the design of high-order arrays associated by exploiting high-order cumulants. The effectiveness of the proposed sparse array design framework is investigated through extensive numerical analysis. A comparative analysis with closed-form solutions and integer linear programming-based array design methods confirms the superiority of the proposed design framework in terms of number of degrees of freedom (DOF) and direction of arrival (DOA) estimation accuracy.

Index Terms—Non-redundant array, minimum-redundant array, sparse array design, integer linear programming.

I. INTRODUCTION

IN recent years, there has been a growing interest in the design and optimization of antenna arrays for various applications, including radar, wireless communication, and navigation [1], [2], [3]. Among different array configurations, sparse arrays have gained significant attention due to their ability to achieve high-resolution with reduced hardware complexity and cost [4],

[5], [6]. Sparse arrays with non-uniform inter-element spacing have the ability to estimate the direction of arrival (DOA) for more sources than the number of physical elements. Typically, resolving more sources is achieved by constructing a virtual array using the second-order or higher-order moments of the received data. The ability to resolve uncorrelated sources is measured by degrees of freedom (DOF), which are related to redundancy for the array. Redundancy, in this context, refers to the existence of overlapping or redundant elements within the virtual array [7]. For a sparse array, lower redundancy corresponds to more degrees of freedom, leading to a greater number of resolvable DOAs.

In the past few decades, various array design methods have been proposed. Given the number of elements, the concepts of non-redundant array (NRA) [8], [9] and minimum-redundant array (MRA) [10] have been proposed to reduce array redundancy. Specifically, NRAs aim to eliminate overlapping virtual elements to create a sparse configuration, whereas MRAs minimize redundant virtual elements while maintaining a virtual uniform linear array (ULA). Although theoretically feasible, solving the above two types of sparse arrays poses considerable challenges.

To facilitate array design, various sparse arrays with closed-form solutions have been proposed. By arranging the array elements in a nested manner, the nested array [11] can provide $\mathcal{O}(N^2)$ DOF with N physical sensors. This significantly enhances the ability to resolve the number of signal sources compared to traditional ULAs, which can distinguish $N - 1$ sources at most. Several extensions have been proposed, e.g., the improved nested array (INA) [12] and the enhanced nested array (ENA) [13], which are achieved by augmenting the inter-element spacing of the external ULA and incorporating additional sensors. Note that although nested arrays and their extended forms can enhance DOF, their difference co-arrays (DCA) maybe not hole-free ULAs, which is necessary for unambiguous and accurate DOA estimation. Another notable type of sparse array is the coprime array (CPA) [14]. CPAs are constructed by arranging multiple subarrays with different numbers of sensors, where the sensor counts are co-prime to each other. Coprime arrays provide enhanced degrees of freedom and increased aperture, leading to improved spatial resolution and direction finding capabilities. Variations of coprime arrays include enhanced coprime array (ECA) [15] and CPA-like array [16], [17], [18], [19], [20], which are specifically designed

Received 14 April 2024; revised 17 August 2024; accepted 1 September 2024. Date of publication 16 September 2024; date of current version 28 October 2024. The work of Yangjingzhi Zhuang, Xuejing Zhang, and Zishu He was supported in part by the National Natural Science Foundation of China under Grant 62101101, Grant 62031007, Grant 62231006, in part by the Sichuan Science and Technology Program under Grant 2024NSFSC1433, and in part by the Peng Cheng Shang Xue Education Fund under Grant XY2021602. The work of Maria Sabrina Greco and Fulvio Gini was supported by the Italian Ministry of Education and Research (MUR) in the framework of the FoReLab project (Departments of Excellence). The associate editor coordinating the review of this article and approving it for publication was Prof. Rodrigo C. de Lamare. (*Corresponding author: Xuejing Zhang.*)

Yangjingzhi Zhuang, Xuejing Zhang, and Zishu He are with the Department of Information and Communication Engineering, University of Electronic Science and Technology of China, Chengdu 611731, China (e-mail: zhuangyangjingzhi@163.com; zhangxuejing@uestc.edu.cn; zshe@uestc.edu.cn).

Maria Sabrina Greco and Fulvio Gini are with the Department of Information Engineering, University of Pisa, 56122 Pisa, Italy (e-mail: maria.greco@unipi.it; fulvio.gini@unipi.it).

Digital Object Identifier 10.1109/TSP.2024.3460383

to augment the DOF and fill in spatial holes. Nevertheless, the aforementioned nested arrays and coprime arrays do not consider the mutual coupling effects between antennas [21]. Additionally, neither type of array allows for flexible design based on practical constraints.

To reduce mutual coupling between antennas, several new forms of sparse arrays have been proposed recently. For example, [22] and [23] introduced the concept of super nested array (SNA), which provides a closed form solution for the sensor location. The augmented nested array (ANA) is presented in [24] to reduce mutual coupling, by splitting the dense subarray of NA into several parts. In [25], a new type of array called thinned co-prime array (TCA) was proposed to reduce mutual coupling. It achieves the same virtual aperture and degrees of freedom as traditional coprime arrays with a smaller number of sensors. In addition, sparse arrays based on the maximum inter-element spacing constraint (MISC) were presented in [26], [27]. It provides a closed-form solution for sparse array design with reduced mutual coupling. In order to obtain high degrees of freedom with low mutual coupling, the enhanced MISC (EMISC) array was proposed in [28]. The fractal arrays were proposed in [29], [30], [31], [32], [33], using the concept of fractal geometry [34]. Fractal arrays can inherit the favorable characteristics of a small array, including low mutual coupling. In addition to considering the mutual coupling effects, recent works have also taken into account the possibility of antenna failures in sparse array design. Specifically, the authors of [35], [36], [37] discussed the robustness and stability of sparse arrays. Several sparse arrays with improved robustness have been presented in [38], [39], [40].

The aforementioned methods focused on sparse array design using second-order difference arrays, whereas several recent works have explored sparse array design using higher-order cumulants [41], [42], aiming to achieve higher DOF. These include studies such as, the $2q$ -level nested arrays ($2q$ L-NA) presented in [43], the simplified and enhanced multiple level nested arrays (SE- $2q$ L-NA) presented in [44], and the fractal array-based $2q$ th order differential cooperative arrays ($2q$ th-O-Fractal) presented in [45], [46]. However, similar to the existing sparse array design methods using second-order cumulants, these approaches are unable to provide flexible array design based on specific requirements, such as array aperture limitations, inter-element spacing constraints, redundancy requirements, and the cumulant order. This motivated us to investigate a general framework for sparse array design, which can achieve flexible sparse array design based on practical considerations.

In this paper, we propose a new framework for sparse array design using integer programming. We find that the design of the non-redundant array and minimum-redundant array can be formulated as an integer linear programming (ILP) problem. On this basis, we can add constraints according to specific requirements, thus resulting in different ILP models and enabling flexible sparse array design. The proposed sparse array design framework allows to impose constraints based on redundancy requirements (such as minimum-redundancy or non-redundancy), as well as consider multiple practical constraints (such as mutual coupling and array aperture limitations)

simultaneously. The proposed scheme can be solved using general-purpose off-the-shelf solvers, such as Gurobi [47] and CPLEX [48]. Moreover, our framework can be extended to higher-order moment scenarios. Previous work utilizing ILP to model sparse array design can be found in [9]. However, the method presented in [9] is only applicable to the design of a non-redundancy array. In contrast, the framework proposed is suitable for the design of both non-redundant arrays and minimum-redundant arrays. Moreover, our framework can be further extended to sparse array design based on higher-order cumulants. Additionally, for the non-redundant array case, the proposed framework utilizes a different modeling approach. The main contributions of this paper can be summarized as follows:

- 1) We propose a new framework for sparse array design utilizing integer linear programming. The proposed scheme can be solved using general-purpose off-the-shelf solvers, providing a new perspective and solution for sparse array design.
- 2) The proposed sparse array design framework allows to impose constraints based on redundancy requirements (such as minimum-redundancy or non-redundancy), as well as considers multiple practical constraints (such as mutual coupling and array aperture limitations) simultaneously.
- 3) The proposed scheme differs from existing ILP-based sparse array design methods and can be extended to array design with higher-order cumulants. Furthermore, the proposed method can achieve multi-objective optimization. For instance, given a fixed number of array elements, it can design a minimum redundancy array while also minimizing mutual coupling.

The paper is organized as follows. In Section II, we review some preliminaries on sparse arrays. In Section III, we propose a new framework to design NRA using integer linear programming. In Section IV, the design of MRA is presented. In Section V, the proposed framework is extended to the designs of NRA and MRA under higher-order cumulants. Numerical results are presented in Section VI to demonstrate the superiority of the proposed framework. Finally, we draw the conclusion in Section VII.

Notations: In this paper, $(\cdot)^T$, $(\cdot)^*$ and $(\cdot)^H$ denote transpose, conjugate and conjugate transpose of matrix or vector, respectively. We use boldface to represent vector \mathbf{a} (lower case) and matrix \mathbf{A} (upper case), respectively. The blackboard bold letter \mathbb{P} represents the collection. \mathbb{Z}_+ represents the set of all positive integers. The cardinality of the collection \mathbb{P} is denoted by $|\mathbb{P}|$. $\mathbb{E}[\cdot]$ is the operation to find the expected value. The vectorization of the matrix \mathbf{A} is expressed as $\text{vec}(\mathbf{A})$. $\|\cdot\|_F$ is the Frobenius norm. $\mathbf{1}_N$ and $\mathbf{0}_N$ denote N -dimensional vector with all elements of one and zero, respectively. \mathbf{I}_N represents the $N \times N$ identity matrix. $j = \sqrt{-1}$ is the imaginary unit. $\text{diag}([a_1, a_2, \dots, a_N])$ returns a diagonal matrix with diagonal elements $\{a_n\}_{n=1}^N$. The Kronecker product and Khatri-Rao product are denoted by \otimes and \odot , respectively. $\mathbf{a} \preceq \mathbf{b}$ and $\mathbf{a} \succeq \mathbf{b}$ are defined as component wise inequality between vectors \mathbf{a} and \mathbf{b} . $\mathbf{a} \sim \mathcal{CN}(\mathbf{0}_N, \Xi)$ indicates that the N -dimensional random

vector \mathbf{a} follows a Gaussian distribution with mean zero and covariance Ξ .

II. PRELIMINARIES

A. Signal Model

Consider K narrowband far-field uncorrelated sources with carrier wavelength λ impinging on an N -element linear array, where the sensor positions are represented by $p_n\lambda/2, n = 1, 2, \dots, N$. Here p_n belongs to an integer set \mathbb{P} ($|\mathbb{P}| = N$) and the position vector is $\mathbf{p} = [p_1, p_2, \dots, p_N]^T$. Without loss of generality, we take $p_1 = 0$. The DOAs of the sources are $\{\theta_1, \dots, \theta_K\}$, with powers $\{\sigma_1^2, \dots, \sigma_K^2\}$, respectively. The array snapshot $\mathbf{x}(t)$ can be expressed as:

$$\mathbf{x}(t) = \sum_{k=1}^K s_k(t)\mathbf{a}(\theta_k) + \mathbf{n}(t) = \mathbf{A}\mathbf{s}(t) + \mathbf{n}(t) \quad (1)$$

where $s_k(t)$ represents the baseband waveform of the k th signal, $\mathbf{n}(t) \sim \mathcal{CN}(\mathbf{0}_N, \zeta^2 \mathbf{I}_N)$ is the noise. Noise and signals are assumed to be uncorrelated. Here, ζ^2 denotes the noise variance. The matrix $\mathbf{A} = [\mathbf{a}(\theta_1), \dots, \mathbf{a}(\theta_K)]$ represents the array manifold with $\mathbf{a}(\theta_k)$ given as:

$$\mathbf{a}(\theta_k) = [1, e^{j\pi p_2 \sin(\theta_k)}, \dots, e^{j\pi p_N \sin(\theta_k)}]^T \quad (2)$$

The spatial covariance matrix of the received data vector $\mathbf{x}(t)$ can be obtained as:

$$\begin{aligned} \mathbf{R}_{\mathbf{x}} &= \mathbb{E}[\mathbf{x}(t)\mathbf{x}^H(t)] = \mathbf{A}\mathbf{R}_{\mathbf{s}}\mathbf{A}^H + \zeta^2 \cdot \mathbf{I}_N \\ &= \sum_{k=1}^K \sigma_k^2 \mathbf{a}(\theta_k)\mathbf{a}^H(\theta_k) + \zeta^2 \cdot \mathbf{I}_N \end{aligned} \quad (3)$$

where $\mathbf{R}_{\mathbf{s}} = \mathbb{E}[\mathbf{s}(t)\mathbf{s}^H(t)] = \text{diag}([\sigma_1^2, \sigma_2^2, \dots, \sigma_K^2])$ is the source covariance matrix. In practice, the covariance $\mathbf{R}_{\mathbf{x}}$ is usually estimated from the sample average of T snapshots.

B. Difference Co-Array

For simplicity, we initially focus on the difference co-array based on the second-order moment. According to (3), the vectorization of $\mathbf{R}_{\mathbf{x}}$ can be expressed as:

$$\mathbf{z} = \text{vec}(\mathbf{R}_{\mathbf{x}}) = (\mathbf{A}^* \odot \mathbf{A})\boldsymbol{\Sigma} + \zeta^2 \cdot \mathbf{e} \quad (4)$$

where $\boldsymbol{\Sigma} = [\sigma_1^2, \sigma_2^2, \dots, \sigma_K^2]^T$ and $\mathbf{e} = \text{vec}(\mathbf{I}_N)$. Comparing (1) and (4), the new vector \mathbf{z} can be regarded as a received signal of a virtual sensor array whose manifold is expressed as $(\mathbf{A}^* \odot \mathbf{A})$. This corresponds to a virtual array, commonly referred to as the difference co-array of the original array. The positions of all virtual array elements can be represented by the following set \mathbb{D} :

$$\mathbb{D} = \{p_i - p_j \mid p_i, p_j \in \mathbb{P}\} \quad (5)$$

For illustration purpose, we introduce the following two definitions.

Definition 1: Given an array \mathbb{P} , the DOF is defined as the cardinality of its difference co-array \mathbb{D} .

Definition 2: The weight function $w(n)$ of an array \mathbb{P} is defined as the number of sensor pairs with interval n , namely,

$$w(n) = \left| \{(p_i, p_j) \in \mathbb{P}^2 \mid p_i - p_j = n\} \right|, \quad n \in \mathbb{D} \quad (6)$$

The performance of correlation-based estimators is primarily influenced by the DOF of the sparse array. A larger DOF allows for the recovery of a greater number of uncorrelated sources. The mutual coupling between array elements can be qualitatively expressed by the weight function. The larger the $w(n)$ corresponding to a small value of n is, the more serious the mutual coupling of the array is. In particular, the first three co-array weights i.e., $w(1)$, $w(2)$ and $w(3)$ have the highest impact on mutual coupling of an array.

III. NON-REDUNDANT LINEAR ARRAY DESIGN

In this section, we present the methodology for designing the non-redundant linear array. Non-redundant arrays maximize the number of DOFs by achieving the maximum possible number of unique elements in the resulting difference co-array. In a non-redundant sparse array, all non-zero co-array elements are distinct. Different from the approach described in [9], we present a new integer linear programming model for designing non-redundant arrays. The proposed framework enables the design of non-redundant arrays under practical constraints.

A. Design of Non-Redundant Linear Arrays

Based on the expression in (5) and the definition of non-redundant array, it is necessary to ensure the uniqueness of all (non-zero) elements in the difference co-array \mathbb{D} to achieve a non-redundant array. It is evident that if the array aperture is sufficiently long, we can always construct a non-redundant array. Therefore, we consider how to minimize the array aperture while ensuring non-redundancy.

Without loss of generality, we assume that the number of antennas is N , and the antennas are arranged in ascending order, i.e., $p_N > p_{N-1} > \dots > p_1$. To facilitate the explanation, we define the following matrix \mathbf{S}_i :

$$\mathbf{S}_i = \begin{bmatrix} -1 & 1 & & & & \\ & -1 & 1 & & & \\ & & & \ddots & & \\ & & & & \ddots & \\ & & & & & -1 & 1 \end{bmatrix} \in \mathbb{R}^{(i-1) \times i} \quad (7)$$

where the subscript i represents the column number of \mathbf{S}_i . Then the ascending order of antenna positions can be constrained by the following inequality:

$$\mathbf{S}_N \mathbf{p} \succeq \mathbf{1}_{N-1} \quad (8)$$

To impose constraints on non-redundancy, we first notice the symmetry of the difference co-array. This allows us to design non-redundant arrays by considering only the positive side of the co-array, thereby reducing computational complexity. To represent the positive co-array from the antenna position vector \mathbf{p} , we define the $U \times N$ combination matrix \mathbf{J} , with $U = N(N-1)/2$. Each row element of \mathbf{J} consists of a positive one and a negative one, thus subtracting the positions of two

antennas at specific locations [9]. Take $N = 4$ as an example, the matrix \mathbf{J} is given by:

$$\begin{bmatrix} -1 & 1 & 0 & 0 \\ -1 & 0 & 1 & 0 \\ -1 & 0 & 0 & 1 \\ 0 & -1 & 1 & 0 \\ 0 & -1 & 0 & 1 \\ 0 & 0 & -1 & 1 \end{bmatrix} \quad (9)$$

Then, the resulting vector \mathbf{Jp} represents all the possible positive elements in \mathbb{D} . To achieve non-redundancy, our main concern is how to ensure the uniqueness of the element values in vector \mathbf{Jp} .

To proceed, we notice that if at most one element of $(\mathbf{Jp} - c \cdot \mathbf{1}_U)$ is zero, it implies no duplicate elements c within the vector \mathbf{Jp} . Based on the above principle, we assume each element value of \mathbf{Jp} does not exceed a positive constant M , and define

$$\mathbf{h} \triangleq [1, 2, \dots, M]^T \quad (10)$$

If for any element c in \mathbf{h} , it is ensured that $(\mathbf{Jp} - c \cdot \mathbf{1}_U)$ has at most one element as zero, then there are no duplicate elements in \mathbf{Jp} . To achieve this, we construct the following vector:

$$\mathbf{1}_M \otimes \mathbf{Jp} - \mathbf{h} \otimes \mathbf{1}_U = \begin{bmatrix} \mathbf{Jp} - 1 \cdot \mathbf{1}_U \\ \mathbf{Jp} - 2 \cdot \mathbf{1}_U \\ \vdots \\ \mathbf{Jp} - M \cdot \mathbf{1}_U \end{bmatrix} \quad (11)$$

Our problem is transformed into how to ensure that there is at most one zero element for each U -dimensional subvector in (11).

The above problem can be modeled and solved by introducing a $UM \times 1$ binary vector \mathbf{b} , whose elements are either 0 or 1. More specifically, given a sufficiently large positive constant α , we constrain \mathbf{p} and \mathbf{b} as

$$-\alpha \cdot \underbrace{\begin{bmatrix} \mathbf{b}_1 \\ \mathbf{b}_2 \\ \vdots \\ \mathbf{b}_M \end{bmatrix}}_{\mathbf{b}} \preceq \underbrace{\begin{bmatrix} \mathbf{Jp} - 1 \cdot \mathbf{1}_U \\ \mathbf{Jp} - 2 \cdot \mathbf{1}_U \\ \vdots \\ \mathbf{Jp} - M \cdot \mathbf{1}_U \end{bmatrix}}_{\mathbf{1}_M \otimes \mathbf{Jp} - \mathbf{h} \otimes \mathbf{1}_U} \preceq \alpha \cdot \underbrace{\begin{bmatrix} \mathbf{b}_1 \\ \mathbf{b}_2 \\ \vdots \\ \mathbf{b}_M \end{bmatrix}}_{\mathbf{b}} \quad (12)$$

In (12), it is important to note that if an element of \mathbf{b} is zero, the corresponding element in $(\mathbf{1}_M \otimes \mathbf{Jp} - \mathbf{h} \otimes \mathbf{1}_U)$ must also be zero. Conversely, if an element of \mathbf{b} is one, there are no restrictions on the values of the elements in the corresponding rows of $(\mathbf{1}_M \otimes \mathbf{Jp} - \mathbf{h} \otimes \mathbf{1}_U)$, as α is sufficiently large.

Recalling (11), to ensure that there is at most one zero element for each U -dimensional subvector, we can constrain the number of ones in \mathbf{b} , resulting in the following compact constraints:

$$(\mathbf{I}_M \otimes \mathbf{1}_U^T) \mathbf{b} \succeq (U - 1) \cdot \mathbf{1}_M \quad (13)$$

$$\mathbf{1}_{UM}^T \mathbf{b} = U(M - 1) \quad (14)$$

The constraint (13) guarantees that there is at most one zero element for each U -dimensional subvector \mathbf{b}_k , $k = 1, \dots, M$. The constraint (14) ensures that the number of zero elements in

Algorithm 1 The NRA Design Algorithm

- 1: **Input:** N , α , M , and $U = N(N - 1)/2$
 - 2: construct \mathbf{S}_N and \mathbf{h} by (7) and (10), respectively
 - 3: construct $U \times N$ combination matrix \mathbf{J} following (9)
 - 4: obtain the model (15) and solve it using ILP solver
 - 5: **Output:** the array elements position vector $\mathbf{p} = [p_1, p_2, \dots, p_N]^T$ and the binary vector \mathbf{b}
-

\mathbf{b} is exactly equal to U . Considering that the length of \mathbf{Jp} is U , the above constraints (12)-(14) ensure that the elements of \mathbf{Jp} are not repeated. In other words, all the (non-zero) elements in the difference co-array \mathbb{D} are unique if (12)-(14) are satisfied.

Finally, the design of non-redundant linear array with minimum array aperture can be formulated as:

$$\underset{\mathbf{p}, \mathbf{b}}{\text{minimize}} \quad p_N \quad (15a)$$

$$\text{subject to} \quad \mathbf{S}_N \mathbf{p} \succeq \mathbf{1}_{N-1} \quad (15b)$$

$$-\alpha \cdot \mathbf{b} \preceq \mathbf{1}_M \otimes \mathbf{Jp} - \mathbf{h} \otimes \mathbf{1}_U \preceq \alpha \cdot \mathbf{b} \quad (15c)$$

$$(\mathbf{I}_M \otimes \mathbf{1}_U^T) \mathbf{b} \succeq (U - 1) \cdot \mathbf{1}_M \quad (15d)$$

$$\mathbf{1}_{UM}^T \mathbf{b} = U(M - 1) \quad (15e)$$

$$\mathbf{b} \in \{0, 1\}^{UM} \quad (15f)$$

$$\mathbf{p} \in \mathbb{Z}_+^N \quad (15g)$$

Note that all the optimization variables in (15) are integers (as indicated in (15f) and (15g)), and the constraints (15b)-(15e) are linear. Therefore, the formulation (15) is an integer linear programming (ILP) problem, which can be solved using general-purpose off-the-shelf solvers, such as Gurobi [47] and CPLEX [48]. The NRA design algorithm is summarized in Algorithm 1.

Remark 1: To ensure that problem (15) has a solution, it is only necessary to take $\alpha \geq M$, and no upper bound is required for α .

B. Design of Generalized Non-Redundant Linear Arrays

In this subsection, we extend the ILP framework in (15) by considering practical constraints. Specifically, we demonstrate the non-redundant array design under array aperture constraint and reduced mutual coupling scenario separately. Its extension to more complicated cases is straightforward.

1) *Desired Array Aperture:* Let A be the desired array aperture for the non-redundant array. Then the problem of non-redundant array design with desired array aperture constraint can be readily formulated by incorporating (15) with the following new constraint:

$$p_N \leq A \quad (16)$$

Since we have already constrained the array aperture, the objective function should naturally become maximizing p_N [9], i.e.,

$$\underset{\mathbf{p}, \mathbf{b}}{\text{maximize}} \quad p_N \quad (17)$$

Also, to ensure the validity of the constraint (16), the range of desired aperture A should be greater than \bar{M} , which represents the array aperture of an N -element non-redundant array with a minimum aperture [9]. In fact, we can find that \bar{M} should be equal to the optimal value of the problem (15). On the other hand, since we are considering the problem of aperture maximization for non-redundant arrays, it is not difficult to infer that there is no upper bound for the desired aperture A .

2) *Reduced Mutual Coupling*: The motivation behind this array design is to mitigate the adverse effects of mutual coupling. Considering the fact that small co-array lag values contribute significantly to the mutual coupling effects, we can constrain the co-array to have holes at lag $1, \dots, L$, where L is a small positive integer. At this point, we have $w(1) = \dots = w(L) = 0$. To accomplish the above objective, we can simply replace constraint (15b) in (15) with the following constraint:

$$\mathbf{S}_N \mathbf{p} \succeq (1 + L) \cdot \mathbf{1}_{N-1} \quad (18)$$

The design process of generalized NRA can be adjusted and modified according to Algorithm 1.

Finally, it should be noted that although both employ integer programming, the proposed framework is different from that in [9]. In particular, the method in [9] designs non-redundant arrays by constraining that each lag is not equal to any of the others. In contrast, our approach directly constrains the occurrences of each lag to achieve non-redundancy. Additionally, it is worth noting that the method in [9] is only applicable to non-redundant arrays, whereas the proposed framework can also be applied to the design of minimum-redundant arrays.

IV. MINIMUM-REDUNDANT LINEAR ARRAY DESIGN

In the previous section, we presented a novel framework based on integer linear programming for the design of non-redundant arrays. In this section, we focus on the design of minimum-redundant arrays using the same framework. Different from the non-redundant arrays, the minimum-redundant arrays provide the lowest possible redundancy while still satisfying specific criteria. Minimum-redundant arrays can be further classified into two types: the restricted MRA and the general MRA.

A. Restricted MRA

In the restricted MRA case, the difference co-arrays are uniformly distributed with intervals of array aperture. In other words, all the elements of the difference co-array \mathbb{D} are consecutive. Under this constraint and given N antennas, the problem is how to minimize the redundancy by designing the position vector $\mathbf{p} = [p_1, p_2, \dots, p_N]^T$.

Following the proposed design framework, we assume that the antennas are arranged in ascending order. Due to the constraint of continuity on the difference co-array, the maximum lag does not exceed $U = N(N - 1)/2$. Based on the above fact, we define $\mathbf{u} = [1, 2, \dots, U]^T$ and introduce a $U^2 \times 1$ binary

vector \mathbf{b} . With a sufficiently large constant α , we constrain \mathbf{p} and \mathbf{b} as:

$$-\alpha \cdot \underbrace{\begin{bmatrix} \mathbf{b}_1 \\ \mathbf{b}_2 \\ \vdots \\ \mathbf{b}_U \end{bmatrix}}_{\mathbf{b}} \preceq \underbrace{\begin{bmatrix} \mathbf{J}\mathbf{p} - 1 \cdot \mathbf{1}_U \\ \mathbf{J}\mathbf{p} - 2 \cdot \mathbf{1}_U \\ \vdots \\ \mathbf{J}\mathbf{p} - U \cdot \mathbf{1}_U \end{bmatrix}}_{\mathbf{1}_U \otimes \mathbf{J}\mathbf{p} - \mathbf{u} \otimes \mathbf{1}_U} \preceq \alpha \cdot \underbrace{\begin{bmatrix} \mathbf{b}_1 \\ \mathbf{b}_2 \\ \vdots \\ \mathbf{b}_U \end{bmatrix}}_{\mathbf{b}} \quad (19)$$

The role of the constraint (19) is similar to (12). Through an appropriate constraint on \mathbf{b} , we can control the redundancy and achieve continuity on the difference co-array.

Specifically, we introduce another binary vector $\mathbf{y} = [y_1, y_2, \dots, y_U]^T$ and constrain \mathbf{b} and \mathbf{y} as:

$$\underbrace{\begin{bmatrix} U(1 - y_1) \\ U(1 - y_2) \\ \vdots \\ U(1 - y_U) \end{bmatrix}}_{U \cdot (\mathbf{1}_U - \mathbf{y})} \preceq \underbrace{\begin{bmatrix} \mathbf{1}_U^T & & & \\ & \mathbf{1}_U^T & & \\ & & \ddots & \\ & & & \mathbf{1}_U^T \end{bmatrix}}_{\mathbf{I}_U \otimes \mathbf{1}_U^T} \underbrace{\begin{bmatrix} \mathbf{b}_1 \\ \mathbf{b}_2 \\ \vdots \\ \mathbf{b}_U \end{bmatrix}}_{\mathbf{b}} \preceq \underbrace{\begin{bmatrix} U - y_1 \\ U - y_2 \\ \vdots \\ U - y_U \end{bmatrix}}_{U \cdot \mathbf{1}_U - \mathbf{y}} \quad (20)$$

From (20), it is not difficult to find that $\mathbf{b}_k = \mathbf{1}_U$, if and only if $y_k = 0$. On the other hand, \mathbf{b}_k contains elements with zero value, if and only if $y_k = 1$. The above conclusions are true for any $k \in \{1, 2, \dots, U\}$. On this basis, we further restrict the elements of \mathbf{y} to be monotonically non-increasing, i.e.,

$$\mathbf{S}_U \mathbf{y} \succeq \mathbf{0} \quad (21)$$

This inequality ensures that the element 1 in the vector \mathbf{y} will be arranged at the front of \mathbf{y} before all zero elements, consequently ensuring the priority arrangement of \mathbf{b}_k with zero elements, thereby preserving the continuity of DCA. With the constraints (20) and (21), the continuity of the difference co-array is guaranteed. Furthermore, to achieve minimal redundancy, we need to maximize the aperture of difference co-array, which is equivalent to maximizing the value of $\mathbf{1}_U^T \mathbf{y}$ or p_N .

Finally, the design of minimum-redundant linear array in the restricted case can be formulated as:

$$\text{maximize}_{\mathbf{p}, \mathbf{b}, \mathbf{y}} \quad \mathbf{1}_U^T \mathbf{y} \quad (22a)$$

$$\text{subject to} \quad \mathbf{S}_N \mathbf{p} \succeq \mathbf{1}_{N-1} \quad (22b)$$

$$\mathbf{S}_U \mathbf{y} \succeq \mathbf{0}_{U-1} \quad (22c)$$

$$-\alpha \mathbf{b} \preceq \mathbf{1}_U \otimes \mathbf{J}\mathbf{p} - \mathbf{u} \otimes \mathbf{1}_U \preceq \alpha \mathbf{b} \quad (22d)$$

$$U \cdot (\mathbf{1}_U - \mathbf{y}) \preceq (\mathbf{I}_U \otimes \mathbf{1}_U^T) \mathbf{b} \preceq U \cdot \mathbf{1}_U - \mathbf{y} \quad (22e)$$

$$\mathbf{1}_{U^2}^T \mathbf{b} = U(U - 1) \quad (22f)$$

$$\mathbf{b} \in \{0, 1\}^{U^2} \quad (22g)$$

$$\mathbf{y} \in \{0, 1\}^U \quad (22h)$$

$$\mathbf{p} \in \mathbb{Z}_+^N \quad (22i)$$

The restricted MRA design algorithm is summarized in Algorithm 2.

Algorithm 2 The Restricted MRA Design Algorithm

- 1: **Input:** N , α , and $U = N(N-1)/2$
- 2: construct $\mathbf{u} = [1, 2, \dots, U]^T$
- 3: construct \mathbf{S}_N and \mathbf{S}_U by (7)
- 4: construct $U \times N$ combination matrix \mathbf{J} following (9)
- 5: obtain the model (22) and solve it using ILP solver
- 6: **Output:** the array elements position vector $\mathbf{p} = [p_1, p_2, \dots, p_N]^T$ and the binary vector \mathbf{b} and \mathbf{y}

B. General MRA

In the general case of MRA, consecutive lags can have a maximum value smaller than the array aperture, but this does not mean that the remaining lags are redundant. The largest lag among consecutive lags is denoted as p_{con} , and it holds that $p_{con} < p_N$.

Similarly, we assume that sensor positions are sorted in an ascending order. Consistent with the restricted MRA case, the binary vector \mathbf{y} is introduced to ensure continuity of difference co-array lags. Besides, M is a sufficiently large positive integer, the same definition as in the zero redundancy problem. Nevertheless, in the general MRA case, not all lags are consecutive. Then the vector \mathbf{y} can no longer be directly constrained with \mathbf{S}_U , but a new weight vector \mathbf{r} is introduced to ensure the continuity of the first few lags:

$$\mathbf{r} = [\beta^{M-1}, \beta^{M-2}, \dots, 1]^T \quad (23)$$

where $\beta > 1$. The vector \mathbf{r} ensures that the elements closer to the beginning of \mathbf{y} carry a heavier weight, aiming to prioritize placing the 1 elements of \mathbf{y} as much as possible at the forefront. This also implies that the elements in $\mathbf{J}\mathbf{p}$ attempt to be as continuous as possible at the beginning. Hence, the general MRA case optimization problem can be formulated as:

$$\text{maximize}_{\mathbf{p}, \mathbf{b}, \mathbf{y}} \quad \mathbf{r}^T \mathbf{y} \quad (24a)$$

$$\text{subject to} \quad \mathbf{S}_N \mathbf{p} \succeq \mathbf{1}_{N-1} \quad (24b)$$

$$-\alpha \mathbf{b} \preceq \mathbf{1}_M \otimes \mathbf{J}\mathbf{p} - \mathbf{h} \otimes \mathbf{1}_U \preceq \alpha \mathbf{b} \quad (24c)$$

$$(\mathbf{I}_M \otimes \mathbf{1}_U^T) \mathbf{b} \preceq U \cdot \mathbf{1}_M - \mathbf{y} \quad (24d)$$

$$\mathbf{1}_{UM}^T \mathbf{b} = U(M-1) \quad (24e)$$

$$\mathbf{b} \in \{0, 1\}^{UM} \quad (24f)$$

$$\mathbf{y} \in \{0, 1\}^M \quad (24g)$$

$$\mathbf{p} \in \mathbb{Z}_+^N \quad (24h)$$

where \mathbf{h} is defined the same as in (15). The general MRA design algorithm is summarized in Algorithm 3.

In contrast to the restricted MRA, the general MRA eliminates the constraint (22c). And in general MRA, the constraint (24d) corresponds to a constraint (22e) in restricted MRA but obviously (24d) is relaxed than (22e). These modifications arise from the fact that the general MRA does not impose strict continuity requirements on the elements of the difference co-array. Rather, it necessitates a more extended initial continuity. To address this, we introduce a weight vector \mathbf{r} aimed at maximizing $\mathbf{r}^T \mathbf{y}$. This ensures that the continuous segment of the

Algorithm 3 The General MRA Design Algorithm

- 1: **Input:** N , α , M , $\beta > 1$ and $U = N(N-1)/2$
- 2: construct \mathbf{h} and \mathbf{r} by (10) and (23), respectively
- 3: construct \mathbf{S}_N by (7)
- 4: construct $U \times N$ combination matrix \mathbf{J} following (9)
- 5: obtain the model (24) and solve it using ILP solver
- 6: **Output:** the array elements position vector $\mathbf{p} = [p_1, p_2, \dots, p_N]^T$ and the binary vector \mathbf{b} and \mathbf{y}

difference co-array for the general minimum-redundant array initiates from the beginning and extends as much as possible.

We also extend the minimum-redundant array to applicative goals, i.e., the MRA design under array aperture constraint and reduced mutual coupling scenario separately. Unlike the NRA, this is ensured by designing the minimum-redundant arrays such that the resulting co-array has one and only one lag with values $1, \dots, L$, where L is a small positive integer:

$$\mathbf{S}_N \mathbf{p} \begin{bmatrix} \mathbf{I}_L & \mathbf{0} \\ \mathbf{0} & \mathbf{0} \end{bmatrix} = \begin{bmatrix} \mathbf{1}_L \\ \mathbf{0}_{N-1-L} \end{bmatrix} \quad (25)$$

and

$$\mathbf{S}_N \mathbf{p} \begin{bmatrix} \mathbf{0} & \mathbf{0} \\ \mathbf{0} & \mathbf{I}_{N-1-L} \end{bmatrix} \preceq \begin{bmatrix} \mathbf{0}_L \\ \mathbf{1}_{N-1-L} \end{bmatrix} \quad (26)$$

Remark 2: It should be noted, for a MRA, the array aperture range is $N \leq M \leq N^2$, $\alpha \geq M$ and no upper bound is required.

Remark 3: In scenarios where the minimum-redundant array is not unique, the proposed algorithm can obtain a minimum-redundant array while minimizing mutual coupling. Taking model (22) as an example, we first note that the number of zero elements in vector \mathbf{b}_1 is equal to $w(1)$. Then, to reduce $w(1)$ and thereby reduce mutual coupling, we can modify the objective function of model (22) as

$$\text{maximize}_{\mathbf{p}, \mathbf{b}, \mathbf{y}} \quad \mathbf{1}_U^T \mathbf{y} + \frac{1}{U+1} \mathbf{1}_U^T \mathbf{b}_1 \quad (27)$$

Note that the coefficient $\frac{1}{U+1}$ plays a trade-off role, allowing for the optimization to first maximize $\mathbf{1}_U^T \mathbf{y}$ and then maximize $\mathbf{1}_U^T \mathbf{b}_1$. Similarly, if we consider $w(1)$, $w(2)$, and $w(3)$, simultaneously, we can reduce mutual coupling by modifying the objective function as

$$\text{maximize}_{\mathbf{p}, \mathbf{b}, \mathbf{y}} \quad \mathbf{1}_U^T \mathbf{y} + \frac{1}{U+1} \mathbf{b}_1 + \frac{1}{(U+1)^2} \mathbf{b}_2 + \frac{1}{(U+1)^3} \mathbf{b}_3 \quad (28)$$

V. NON-REDUNDANT AND MINIMUM-REDUNDANT LINEAR SPARSE ARRAY DESIGN WITH $2q$ TH-ORDER CUMULANTS

In this section, we extend the proposed framework to handle $2q$ th-order cumulants. Recently, these algorithms have been further expanded to process arbitrary even-order ($2q$) cumulants of the data, leading to a new family of DOA estimation algorithms known as the $2q$ MUSIC methods. It has been demonstrated that the identifiability, resolution performance, and robustness of these $2q$ MUSIC algorithms improve with increasing q , thereby

enhancing the processing capabilities of $2q$ th-order cumulant-based methods. The higher performance of these $2q$ MUSIC methods can be due to a deeper connection between the $2q$ th-order cumulants and the higher-order virtual array, which effectively behaves like a much longer array compared to the physical array. Sections II-IV are all based on difference co-arrays, which are primarily related to second-order cumulants. However, by considering $2q$ th-order difference co-arrays, we can effectively deal with $2q$ th-order cumulants.

A. $2q$ th-Order Circular Cumulants and Difference Co-Array

The signal model has been introduced in Equation (1). The $2q$ th-order circular cumulants of the signal vector $\mathbf{x}(t)$ with orientation u ($u \in [0, q-1]$) is

$$\begin{aligned} \mathbf{C}_{2q,\mathbf{x}}(u) &= \sum_{k=1}^K c_{2q,s_k} \left[\mathbf{a}(\theta_k)^{\otimes u} \otimes \mathbf{a}(\theta_k)^{* \otimes (q-u)} \right] \\ &\times \left[\mathbf{a}(\theta_k)^{\otimes u} \otimes \mathbf{a}(\theta_k)^{* \otimes (q-u)} \right]^H + \sigma_u^2 \mathbf{I}_{N^q} \cdot \delta(q-1) \end{aligned} \quad (29)$$

where the noise power is denoted by σ_u^2 and the vector $\mathbf{a}(\theta_k)^{\otimes u}$ is defined as $\mathbf{a}(\theta_k)$ with the Kronecker product \otimes utilized $u-1$ times.

Then vectorizing the cumulant matrix $\mathbf{C}_{2q,\mathbf{x}}(u)$, we get the array manifold of $2q$ th-order virtual array:

$$\mathbf{V}(\boldsymbol{\theta}) = [\mathbf{v}(\theta_1), \mathbf{v}(\theta_2), \dots, \mathbf{v}(\theta_K)] \quad (30)$$

where

$$\begin{aligned} \mathbf{v}(\theta_k) &= \left[\mathbf{a}(\theta_k)^{\otimes u} \otimes \mathbf{a}(\theta_k)^{* \otimes (q-u)} \right]^* \\ &\otimes \left[\mathbf{a}(\theta_k)^{\otimes u} \otimes \mathbf{a}(\theta_k)^{* \otimes (q-u)} \right] \end{aligned} \quad (31)$$

The distinct columns of \mathbf{V} act as the virtual array manifold of an extended array aperture. As proved in [43], $\mathbf{v}(\theta_k)$ is independent of the orientation u . The positions of this virtual array is termed as the $2q$ th-order difference co-array of the original array and can be represented by the set \mathbb{D}_q , which can be expressed as:

$$\mathbb{D}_q = \left\{ \sum_{i=1}^q p_{n_i} - \sum_{j=q+1}^{2q} p_{n_j} \mid p_{n_i}, p_{n_j} \in \mathbb{P} \right\} \quad (32)$$

where p_{n_i} and p_{n_j} take values from the set of physical array positions \mathbb{P} .

In the context of an N -sensor physical array, the $2q$ th-order difference co-array \mathbb{D}_q contains a maximum of N^{2q} lags, accounting for redundancies. Consequently, the cardinality of \mathbb{D}_q is bounded by $\mathcal{O}(N^{2q})$, signifying that no array can possess more elements in its $2q$ th-order difference co-array than this upper limit.

B. ILP Framework With $2q$ th-Order Difference Co-Array

In contrast to the case of $q=1$, when $q \geq 2$, it is necessary to consider all possible $2q$ th-order difference co-array lags, even though the $2q$ th-order difference co-array is inherently symmetric around lag 0. This complexity arises when $q \geq 2$,

as the arrangement of lags becomes more intricate, making it difficult to determine which lags are positive without knowing the exact positions of the array elements.

First, let's deconstruct \mathbb{D}_q :

$$\begin{aligned} \mathbb{D}_q &= \left\{ \sum_{i=1}^q p_{n_i} - \sum_{j=q+1}^{2q} p_{n_j} \mid p_{n_i}, p_{n_j} \in \mathbb{P} \right\} \\ &= \left\{ p_{n_i} - p_{n_j} + \sum_{i=1}^{q-1} p_{n_i} - \sum_{j=q+1}^{2q-1} p_{n_j} \mid p_{n_i}, p_{n_j} \in \mathbb{P} \right\} \end{aligned} \quad (33)$$

Hence, a new matrix $\mathbf{G}_q \in \mathbb{R}^{E_q \times N}$ is constructed to guarantee that $\mathbf{G}_q \mathbf{p}$ contains all possible $2q$ th-order difference co-array lags. And we define a matrix $\mathbf{\Gamma}_q \in \mathbb{R}^{F_q \times N}$ that contains all the difference co-array lags, except for repeated vectors, i.e., we remove the redundant row vectors in \mathbf{G}_q , $\mathbf{\Gamma}_q \triangleq \text{unique}(\mathbf{G}_q)$. When $q=1$, we have

$$\mathbf{G}_1 = \begin{bmatrix} -\mathbf{J} \\ \mathbf{J} \\ \mathbf{0}^T \\ \vdots \\ \mathbf{0}^T \end{bmatrix} \in \mathbb{R}^{E_1 \times N} \quad \mathbf{\Gamma}_1 = \begin{bmatrix} -\mathbf{J} \\ \mathbf{J} \\ \mathbf{0}^T \end{bmatrix} \in \mathbb{R}^{F_1 \times N} \quad (35)$$

where $E_1 = N^2$. Hence, combining (34), when $q=2$, we have

$$\mathbf{G}_2 = \mathbf{1}_{F_1} \otimes \mathbf{\Gamma}_1 + \mathbf{\Gamma}_1 \otimes \mathbf{1}_{F_1} \in \mathbb{R}^{E_2 \times N} \quad (36)$$

where $E_2 = F_1^2$. Then we remove the redundant row vectors in \mathbf{G}_2 to get $\mathbf{\Gamma}_2 \in \mathbb{R}^{F_2 \times N}$. And when $q=3$, we can know:

$$\mathbf{G}_3 = \mathbf{1}_{F_2} \otimes \mathbf{\Gamma}_1 + \mathbf{\Gamma}_2 \otimes \mathbf{1}_{F_1} \in \mathbb{R}^{E_3 \times N} \quad (37)$$

where $E_3 = F_1 F_2$. Similarly, by removing the redundant row vectors in \mathbf{G}_3 to get $\mathbf{\Gamma}_3 \in \mathbb{R}^{F_3 \times N}$. Then it is not difficult to extend to the case where $q > 2$:

$$\mathbf{G}_q = \mathbf{1}_{F_{q-1}} \otimes \mathbf{\Gamma}_1 + \mathbf{\Gamma}_{q-1} \otimes \mathbf{1}_{F_1} \in \mathbb{R}^{E_q \times N} \quad (38)$$

where $E_q = F_1 F_{q-1}$. Likewise, by removing the redundant row vectors in \mathbf{G}_q to get $\mathbf{\Gamma}_q \in \mathbb{R}^{F_q \times N}$, i.e., $\mathbf{\Gamma}_q \triangleq \text{unique}(\mathbf{G}_q)$.

Moreover, the symmetry still exists in higher order cumulants, only positive lags need to be considered. Hence, we define $F_{q+} = (F_q - 1)/2$ to simplify the expression. Thus, a form of the ILP optimization problem for extracting non-redundant arrays can be given as:

$$\text{minimize}_{\mathbf{p}, \mathbf{b}} \quad p_N \quad (39a)$$

$$\text{subject to} \quad \mathbf{S}_N \mathbf{p} \succeq \mathbf{1}_{N-1} \quad (39b)$$

$$-\alpha \mathbf{b} \preceq \mathbf{1}_M \otimes \mathbf{\Gamma}_q \mathbf{p} - \mathbf{h} \otimes \mathbf{1}_{F_q} \preceq \alpha \mathbf{b} \quad (39c)$$

$$(\mathbf{I}_M \otimes \mathbf{1}_{F_q}^T) \mathbf{b} \succeq (F_q - 1) \cdot \mathbf{1}_M \quad (39d)$$

$$\mathbf{1}_{F_q M}^T \mathbf{b} = F_q M - F_{q+} \quad (39e)$$

$$\mathbf{b} \in \{0, 1\}^{F_q M} \quad (39f)$$

$$\mathbf{p} \in \mathbb{Z}_+^N \quad (39g)$$

Algorithm 4 The $2q$ th-Order NRA Design Algorithm

- 1: **Input:** N , α , M , and q
- 2: construct \mathbf{S}_N and \mathbf{h} by (7) and (10), respectively
- 3: construct \mathbf{G}_q by (38) and $\Gamma_q \triangleq \text{unique}(\mathbf{G}_q)$
- 4: obtain the model (39) and solve it using ILP solver
- 5: **Output:** the array elements position vector $\mathbf{p} = [p_1, p_2, \dots, p_N]^T$ and the binary vector \mathbf{b}

The ILP optimization problem for minimum-redundant arrays in the restricted case is formulated in the following form:

$$\text{maximize}_{\mathbf{p}, \mathbf{b}, \mathbf{y}} \mathbf{1}_{F_{q+}}^T \mathbf{y} \quad (40a)$$

$$\text{subject to } \mathbf{S}_N \mathbf{p} \succeq \mathbf{1}_{N-1} \quad (40b)$$

$$\mathbf{S}_{F_{q+}} \mathbf{y} \succeq \mathbf{0}_{F_{q+}-1} \quad (40c)$$

$$-\alpha \mathbf{b} \preceq \mathbf{1}_{F_q} \otimes \Gamma_q \mathbf{p} - \mathbf{u}_q \otimes \mathbf{1}_{F_q} \preceq \alpha \mathbf{b} \quad (40d)$$

$$F_q \cdot (\mathbf{1}_{F_{q+}} - \mathbf{y}) \preceq (\mathbf{I}_{F_{q+}} \otimes \mathbf{1}_{F_q}^T) \mathbf{b} \quad (40e)$$

$$(\mathbf{I}_{F_{q+}} \otimes \mathbf{1}_{F_q}^T) \mathbf{b} \preceq F_q \cdot \mathbf{1}_{F_{q+}} - \mathbf{y} \quad (40f)$$

$$\mathbf{1}_{F_{q+}F_q}^T \mathbf{b} = F_q F_{q+} - F_{q+} \quad (40g)$$

$$\mathbf{b} \in \{0, 1\}^{F_q F_{q+}} \quad (40h)$$

$$\mathbf{y} \in \{0, 1\}^{F_{q+}} \quad (40i)$$

$$\mathbf{p} \in \mathbb{Z}_+^N \quad (40j)$$

where $\mathbf{u}_q = [1, 2, \dots, F_{q+}]^T$.

The general case optimization problem for minimum-redundant arrays can be formulated as:

$$\text{maximize}_{\mathbf{p}, \mathbf{b}, \mathbf{y}} \mathbf{r}^T \mathbf{y} \quad (41a)$$

$$\text{subject to } \mathbf{S}_N \mathbf{p} \succeq \mathbf{1}_{N-1} \quad (41b)$$

$$-\alpha \mathbf{b} \preceq \mathbf{1}_M \otimes \Gamma_q \mathbf{p} - \mathbf{h} \otimes \mathbf{1}_{F_q} \preceq \alpha \mathbf{b} \quad (41c)$$

$$(\mathbf{I}_M \otimes \mathbf{1}_{F_q}^T) \mathbf{b} \preceq F_q \cdot \mathbf{1}_M - \mathbf{y} \quad (41d)$$

$$\mathbf{1}_{F_q M}^T \mathbf{b} = F_q M - F_{q+} \quad (41e)$$

$$\mathbf{b} \in \{0, 1\}^{F_q M} \quad (41f)$$

$$\mathbf{y} \in \{0, 1\}^M \quad (41g)$$

$$\mathbf{p} \in \mathbb{Z}_+^N \quad (41h)$$

where $\mathbf{r} = [\beta^{H-1}, \beta^{H-2}, \dots, 1]^T$, $\beta > 1$.

The design algorithm flow of the $2q$ th-order NRA is summarized in Algorithm 4. The design flow of the $2q$ th-order MRA can be obtained by combining (40) and (41) and modifying it with reference to Algorithm 4. In addition, their generalized arrays can also be adjusted and modified with reference to the second-order case.

Comparing the array design framework when $q = 1$ to the framework when $q \geq 2$, it is evident that the latter become more complex. However, by simply adapting the matrix used to generate difference co-array elements, the design framework can be extended to higher-order arrays. This indicates that our array design can be readily extended to higher-order arrays, a proposition substantiated by subsequent simulations that confirmed its effectiveness.

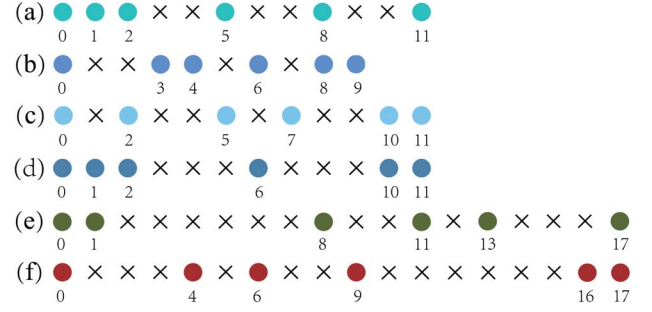


Fig. 1. Array structures of different types of 6-element sparse arrays under consideration. (a) Nested array. (b) Co-prime array. (c) Super nested array. (d) MISC array. (e) Optimized non-redundant array. (f) Proposed non-redundant array.

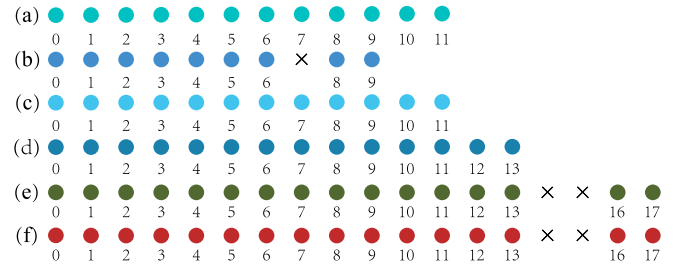


Fig. 2. Difference co-arrays of different types of 6-element sparse arrays. (a) Nested array. (b) Co-prime array. (c) Super nested array. (d) MISC array. (e) Optimized non-redundant array. (f) Proposed non-redundant array.

VI. SIMULATION RESULTS

In this section, we provide numerical examples to illustrate the superiority of the proposed array designs in terms of number of DOFs, weight functions, DOA estimation performance, and mutual coupling effects compared to popular array structures of nested array (NA) [11], co-prime array (CPA) [14], super nested array (SNA) [22], MISC array [26] and optimized non-redundant array (ONRA) [9]. In our simulations, we use Gurobi [47] to solve the ILP models¹.

A. Non-Redundant Linear Sparse Array

In the first simulation example, we compare the performance of the proposed NRA (PNRA), NA, CPA, SNA, ONRA and MISC array. Each of these arrays contains 6 elements, and their distribution and DCAs are shown in Figs. 1 and 2, respectively.

From Fig. 2, we notice that the DCAs of some arrays are not hole-free, so it is necessary to use the array interpolation method [49] to fill the holes first, and then use the MUSIC algorithm for DOA estimation. Moreover, in subsequent simulations, we use the relaxed optimization framework to obtain a simulated hole-free array. For details, please refer to Equation (44) of [9]. In the framework, the regularization parameter in the array interpolation algorithm are uniformly set to 0.25.

We compare the DOA estimation performance of all the arrays under consideration. The scenario involves six sensors and

¹The MATLAB codes for the proposed method are available online at <https://zhangxuejing7.github.io/HomePage/>.

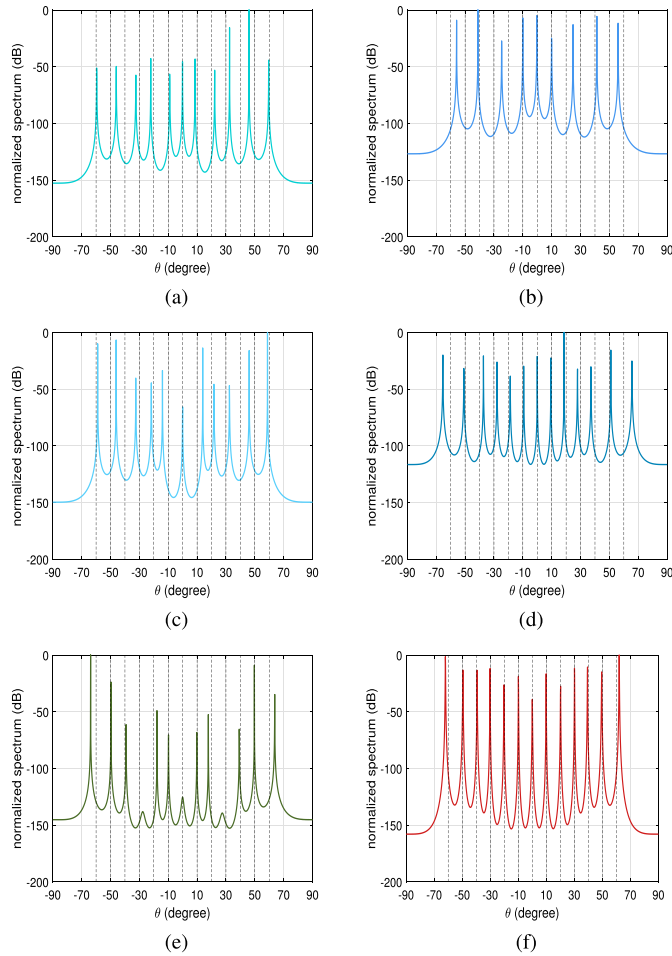


Fig. 3. The MUSIC spectra for different types of 6-element sparse arrays. $Q = 13$ sources uniformly distributed in $[-60^\circ, 60^\circ]$, the number of snapshots N_s is 500, SNR is 0 dB. (a) Nested array. (b) Co-prime array. (c) Super nested array. (d) MISC array. (e) Optimized non-redundant array. (f) Proposed non-redundant array.

$Q = 13$ sources uniformly distributed in $[-60^\circ, 60^\circ]$. We set the number of snapshots N_s to 500 and the input signal-to-noise ratio (SNR) to 0 dB. And $\text{SNR} = 20 \log_{10}(\text{Power}_s / \text{Power}_n)$, which Power_s and Power_n are the power of signal and of noise, respectively. Mutual coupling among the sensors is ignored in this subsection.

Fig. 3 shows the MUSIC spectra for NA, CPA, SNA, MISC, ONRA and PNRA, respectively. It is evident that the first three arrays are unable to fully identify the thirteen signal sources due to their limited DOF. In contrast, the remaining arrays successfully identify all the sources. In addition, it should be noted that although the difference co-array of the proposed non-redundant array is the same as that of the optimized non-redundant array (see Fig. 2(e) and 2(f)), the MUSIC spectra of the two methods are different. This reason is that their original array distributions (see Fig. 1(e) and 1(f)) are different. We use the data received by the original array for covariance reconstruction, and different array distributions naturally correspond to different MUSIC spectra.

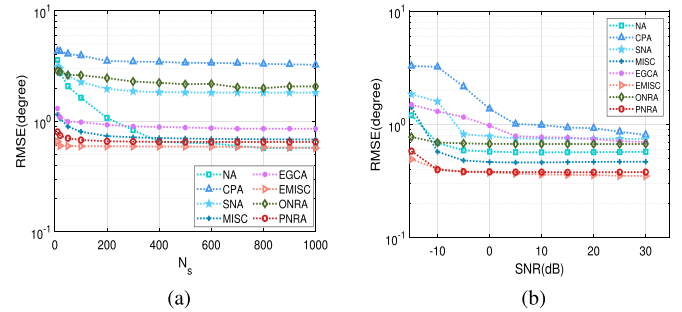


Fig. 4. RMSE of DOA estimates. $Q = 3$ sources are located at $[-5^\circ, 0^\circ, 7^\circ]$. (a) RMSE versus the number of snapshots (N_s). SNR is 0 dB. (b) RMSE versus SNR. The number of snapshots N_s is 500.

The results of the root mean squared error (RMSE) for various arrays, are shown in Fig. 4, which is based on 1000 Monte Carlo trials. In our simulations, we considered three signal sources, with true DOA set at $-5^\circ, 0^\circ$ and 7° , respectively. In addition, for a more comprehensive comparison, we also added the EGCA [20] and EMISC [28] for comparison. Their array element position vectors \mathbf{p} are $[0, 1, 2, 6, 7, 10, 13]^T$ and $[0, 3, 5, 7, 12, 20, 28, 30, 31, 34]^T$. Due to the composition rules, EGCA consists of at least 7 array elements and EMISC consists of at least 10 array elements, so we will not compare them in terms of degrees of freedom and difference co-arrays. Fig. 4(a) illustrates the variation of RMSE as a function of the numbers of snapshots while $\text{SNR} = 0$ dB. Notably, the RMSE for all arrays consistently reduces as the N_s increases. Remarkably, the proposed array exhibits consistently low RMSE. This observation is further reinforced by Fig. 4(b), which depicts the RMSE as a function of the SNR while $N_s = 500$.

B. Generalized Non-Redundant Linear Sparse Array

In this subsection, we analyze the DOA estimation performance of generalized NRA. For comparison, we select [9] as the benchmark, given that arrays like NA lack the capabilities of achieving the desired aperture and reduced mutual coupling. The number of data snapshots and the fixed SNR remain at 500 and 0 dB, respectively.

We consider three cases, namely the proposed non-redundant array with desired aperture (PNRA_{da}), reduced mutual coupling (PNRA_{mc}), and the hybrid NRA (PNRA_{hy}), corresponding to ONRA_{da}, ONRA_{mc} and ONRA_{hy} proposed in [9]. In the simulations, we set the desired aperture A to 25 and the parameter L related to reducing mutual coupling to 1. The distribution and DCAs of these arrays are shown in Figs. 5 and 6, respectively. It can be seen from Fig. 6 that $w(1)$ of the NRA with reduced mutual coupling and the hybrid NRA no longer exists.

Figs. 7–9 show the MUSIC spectra of generalized non-redundant linear sparse arrays. The solid lines represent the results obtained without considering mutual coupling, whereas the blue dotted lines represent the results when mutual coupling is taken into account with $|c_1| = 0.5$. $|c_1|$ is the coupling coefficient between two array elements with a distance of $\lambda/2$ and $|c_i|/|c_j| = j/i$.

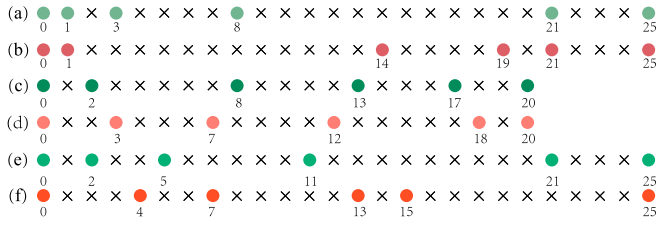


Fig. 5. Array structures of different types of 6-element generalized non-redundant linear sparse arrays. (a) Optimized non-redundant array with desired aperture. (b) Proposed non-redundant array with desired aperture. (c) Optimized non-redundant array with reduced mutual coupling. (d) Proposed non-redundant array with reduced mutual coupling. (e) Optimized hybrid non-redundant array. (f) Proposed hybrid non-redundant array.

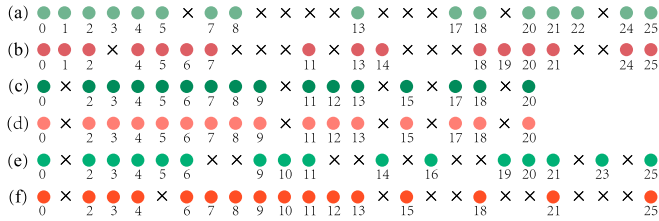


Fig. 6. Difference co-arrays of different types of generalized non-redundant linear sparse arrays. (a) Optimized non-redundant array with desired aperture. (b) Proposed non-redundant array with desired aperture. (c) Optimized non-redundant array with reduced mutual coupling. (d) Proposed non-redundant array with reduced mutual coupling. (e) Optimized hybrid non-redundant array. (f) Proposed hybrid non-redundant array.

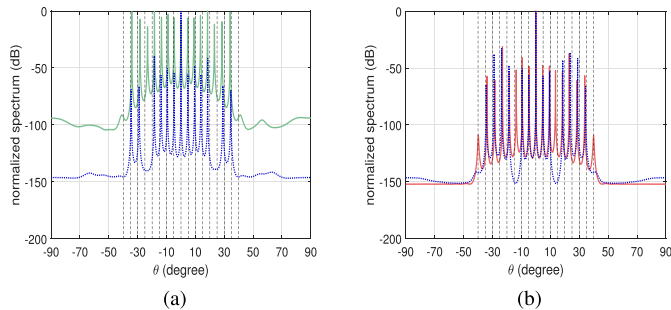


Fig. 7. The MUSIC spectra for different types of 6-element generalized non-redundant linear sparse arrays. $Q = 17$ sources uniformly distributed in $[-40^\circ, 40^\circ]$, the number of snapshots N_s is 500, SNR is 0 dB. (a) Optimized non-redundant array with desired aperture. (b) Proposed non-redundant array with desired aperture.

In Fig. 7(a) and 7(b), we present the angle estimation results for a non-redundant array with the desired aperture. The scenario consists of $Q = 17$ sources uniformly distributed within the angular range $[-40^\circ, 40^\circ]$. From the figures, it is evident that both ONRAda and PNRAda successfully separate all 17 signal sources. Nevertheless, when considering the influence of mutual coupling, both arrays experience missed detections, resulting in a reduced number of resolvable signal sources.

In Fig. 8(a) and 8(b), we present a comparison of the DOA estimation performance between ONRAmc and PNRAmc. The scenario includes $Q = 13$ sources uniformly distributed within the angular range $[-48^\circ, 48^\circ]$. Both arrays successfully identify

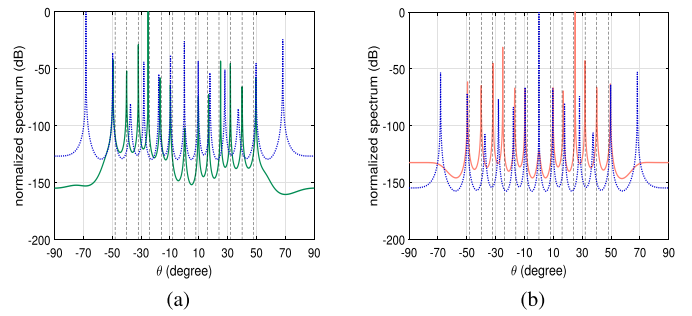


Fig. 8. The MUSIC spectra for different types of 6-element generalized non-redundant linear sparse arrays. $Q = 13$ sources uniformly distributed in $[-48^\circ, 48^\circ]$, the number of snapshots N_s is 500, SNR is 0 dB. (a) Optimized non-redundant array with reduced mutual coupling. (b) Proposed non-redundant array with reduced mutual coupling.

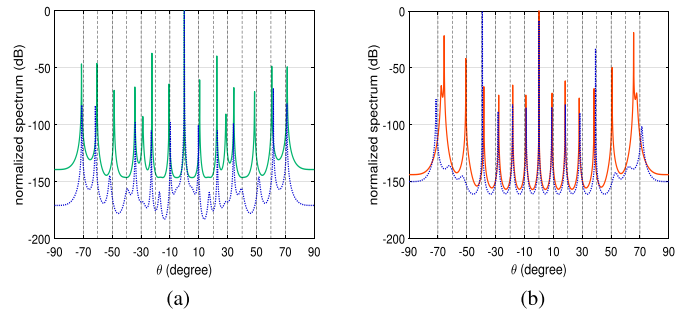


Fig. 9. The MUSIC spectra for different types of 6-element generalized non-redundant linear sparse arrays. $Q = 15$ sources uniformly distributed in $[-70^\circ, 70^\circ]$, the number of snapshots N_s is 500, SNR is 0 dB. (a) Optimized hybrid non-redundant array. (b) Proposed hybrid non-redundant array.

all 13 sources, although when mutual coupling is taken into account, the DOA estimation accuracy of the arrays is noticeably reduced.

Similar trends are observed for ONRAhy and PNRAhy, as shown in Fig. 9(a) and 9(b), respectively. In this simulation, there are 15 signal sources evenly distributed across the range of $[-70^\circ, 70^\circ]$. Even though the accuracy of DOA estimation decreases significantly when mutual coupling is considered, both arrays are capable of detecting all 15 sources.

In Fig. 10, the variation of DOA estimation RMSE as a function of the mutual coupling coefficient of the three generalized NRAs is shown under the conditions of SNR = 0dB and $N_s = 500$. The signal sources in Fig. 10(a) are close, with angles of 0° and 6° respectively. We can find that the arrays ONRAmc, ONRAhy, PNRAmc, and PNRAhy with $w(1) = 0$ have lower RMSE than ONRAda and PNRAda with unconstrained mutual coupling. In Fig. 10(b), there are five signal sources spaced far apart, with angles evenly distributed in $[-20^\circ, 20^\circ]$. Similarly, ONRAmc, ONRAhy, PNRAmc, and PNRAhy have lower RMSE than ONRAda and PNRAda. This shows that our operation to reduce the influence of mutual coupling is effective.

Table I presents the weight function analysis of generalized NRA. The values of $w(2)$ for all six arrays are consistently 1. However, in the four arrays designed to reduce mutual coupling,

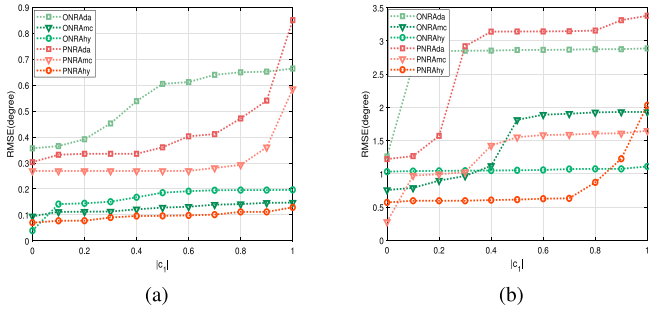


Fig. 10. RMSE of DOA estimates. The number of snapshots N_s is 500, SNR is 0 dB. (a) RMSE versus $|c_1|$ with two sources at $[0^\circ, 6^\circ]$. (b) RMSE versus $|c_1|$ with five sources at $[-20^\circ, -10^\circ, 0^\circ, 10^\circ, 20^\circ]$.

TABLE I
WEIGHT FUNCTION COMPARISON OF DIFFERENT ARRAYS

Arrays	$w(1)$	$w(2)$
ONRAda	1	1
PNRAda	1	1
ONRAmc	0	1
PNRAmc	0	1
ONRAhy	0	1
PNRAhy	0	1

the values of $w(1)$ are uniformly zero. This substantiates the effectiveness of our framework.

C. Minimum-Redundant Linear Sparse Array

In this subsection, we conduct simulations to compare the DOA estimation performance of the MRA and its generalized array design framework proposed in this paper. The concept of MRA encompasses two definitions: MRA under restricted case (PMRAr) and general case (PMRAg). As with the generalized non-redundant array, we consider three scenarios for the MRA: the MRA with desired aperture (PMRArda, PMRAgda), the MRA with reduced mutual coupling (PMRArmc, PMRAgmc), and the hybrid MRA (PMRArhy, PMRAghy), satisfying the first two requirements simultaneously.

In the simulation, we set the desired array aperture to 10 for the restricted MRA, and 16 for the general MRA. All the decoupling-related parameters L are set to 2. The configurations of MRA, its generalized array, and the difference co-array are shown in Figs. 11 and 12, respectively.

Then, we compare the DOA estimation performance of MRAs, and the corresponding MUSIC spectrum is shown in Fig. 13. In this simulation, we utilized 9 signal sources evenly distributed within $[-60^\circ, 60^\circ]$, with $N_s = 500$, and $\text{SNR} = 0$ dB. As observed from Fig. 13, all arrays identify 9 sources. However, the performance of restricted MRA outperforms that of general MRA. For instance, while PMRAg, PMRAgda, and PMRAgmc can distinguish all signal sources, they exhibit significant errors. Additionally, PMRAghy even introduced a false signal source. These limitations stem from the discontinuous DCA in the general MRA, rendering it unsuitable for direct DOA estimation using the MUSIC algorithm. As previously

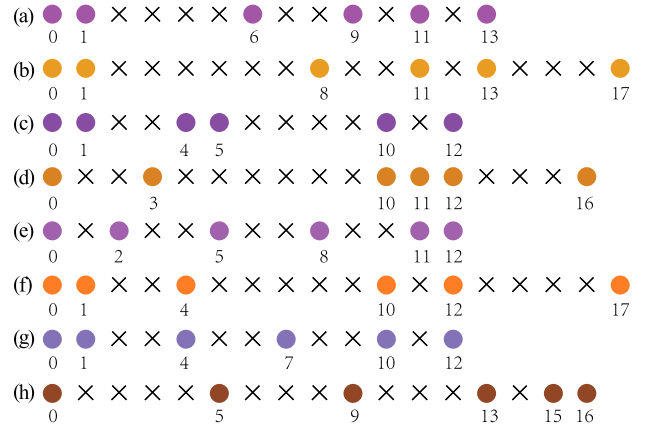


Fig. 11. Array structures of different types of MRA and generalized MRA. (a) Proposed minimum-redundant array under restricted case. (b) Proposed minimum-redundant array under general case. (c) Proposed minimum-redundant array under restricted case with desired aperture. (d) Proposed minimum-redundant array under general case with desired aperture. (e) Proposed minimum-redundant array under restricted case with reduced mutual coupling. (f) Proposed minimum-redundant array under general case with reduced mutual coupling. (g) Proposed hybrid minimum-redundant array under restricted case. (h) Proposed hybrid minimum-redundant array under general case.

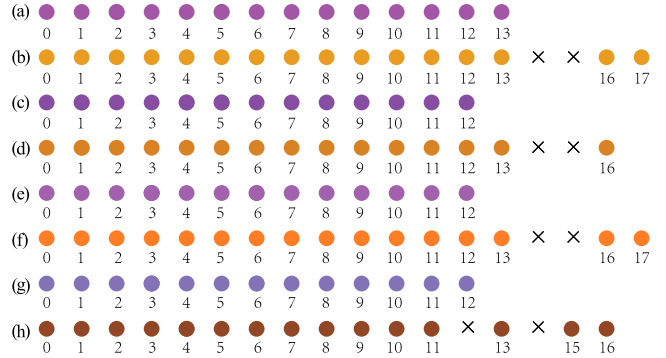


Fig. 12. Difference co-arrays of different types of MRA and generalized MRA. (a) Proposed minimum-redundant array under restricted case. (b) Proposed minimum-redundant array under general case. (c) Proposed minimum-redundant array under restricted case with desired aperture. (d) Proposed minimum-redundant array under general case with desired aperture. (e) Proposed minimum-redundant array under restricted case with reduced mutual coupling. (f) Proposed minimum-redundant array under general case with reduced mutual coupling. (g) Proposed hybrid minimum-redundant array under restricted case. (h) Proposed hybrid minimum-redundant array under general case.

mentioned, we employed an array interpolation algorithm to address the holes in the DCA, leading to errors in the DOA estimation. For the same reason, a longer virtual array aperture does not necessarily imply an improved estimation accuracy.

In Fig. 14, we investigate the relationship between the DOA estimation performance of MRAs and the coupling coefficient $|c_1|$. We consider two distinct scenarios: the first one involves two signal sources located close to each other at angles 0° and 6° , as shown in Fig. 14(a). The second one comprises five signal sources widely distributed within the range of $[-20^\circ, 20^\circ]$, as depicted in Fig. 14(b). For both scenarios, we employ 500 snapshots and set the SNR to 0 dB.

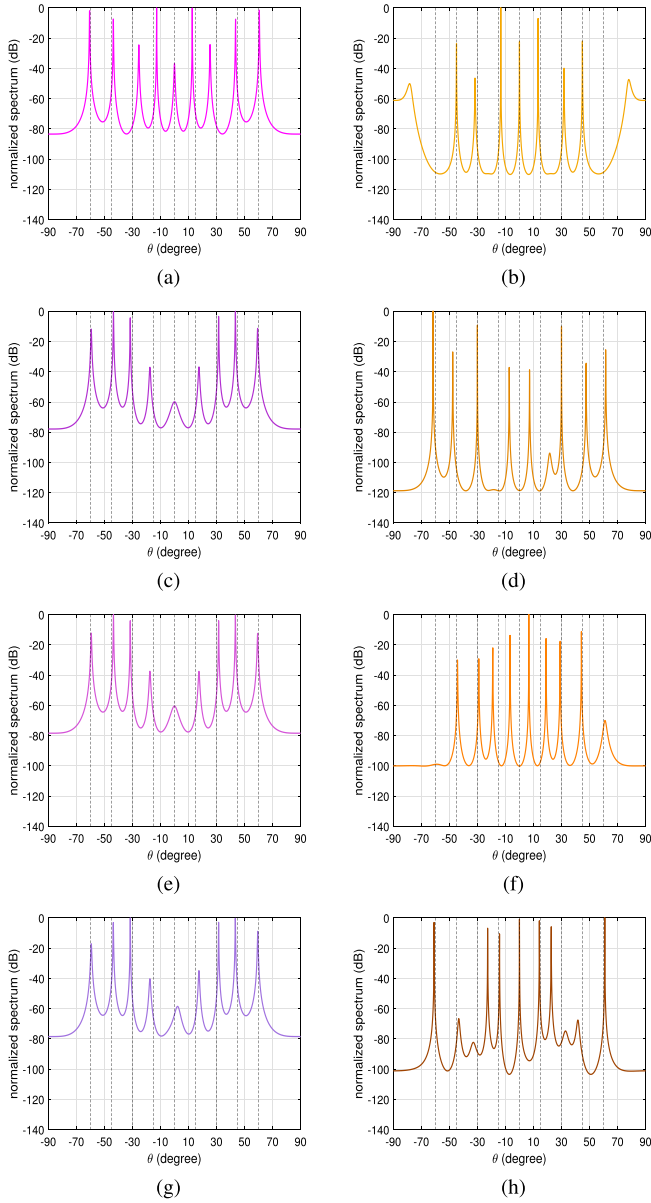


Fig. 13. The MUSIC spectra for different types of MRA and generalized MRA. $Q = 13$ sources uniformly distributed in $[-60^\circ, 60^\circ]$, the number of snapshots N_s is 500, SNR is 0 dB. (a) Proposed minimum-redundant array under restricted case. (b) Proposed minimum-redundant array under general case. (c) Proposed minimum-redundant array under restricted case with desired aperture. (d) Proposed minimum-redundant array under general case with desired aperture. (e) Proposed minimum-redundant array under restricted case with reduced mutual coupling. (f) Proposed minimum-redundant array under general case with reduced mutual coupling. (g) Proposed hybrid minimum-redundant array under restricted case. (h) Proposed hybrid minimum-redundant array under general case.

From Fig. 14(a), it is evident that when signal sources are in close proximity, the RMSE of all restricted MRAs is smaller than that of general MRA. This observation indicates that restrict MRAs exhibit superior performance when the signal sources are close. Additionally, after decoupling processing, the RMSE of PMRArm and PMRArhy is improved compared to PMRAr and PMRArda, which aligns with the trends observed in general MRAs. In Fig. 14(b), the performance of PMRAgmc

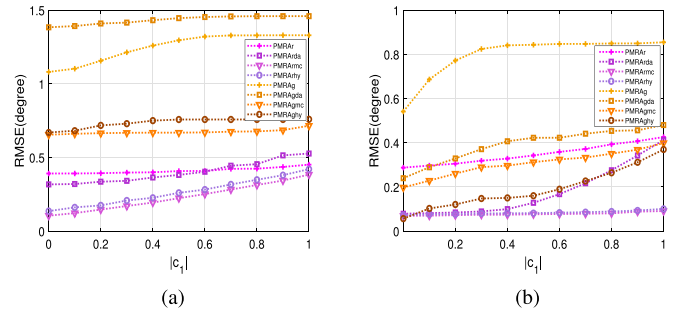


Fig. 14. RMSE of DOA estimates. The number of snapshots N_s is 500, SNR is 0 dB. (a) RMSE versus $|c_1|$ with two sources at $[0^\circ, 6^\circ]$. (b) RMSE versus $|c_1|$ with five sources at $[-20^\circ, -10^\circ, 0^\circ, 10^\circ, 20^\circ]$.

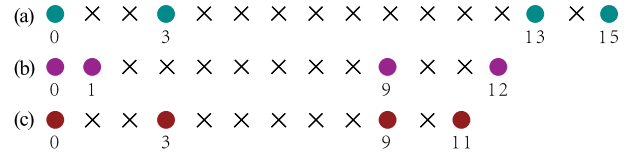


Fig. 15. Array structures of different types of 4-element $2q$ -level non-redundant and minimum-redundant linear sparse arrays ($q = 2$). (a) Proposed $2q$ -level non-redundant array. (b) Proposed $2q$ -level minimum-redundant array under restricted case. (c) Proposed $2q$ -level minimum-redundant array under general case.

and PMRAghy is better than that of PMRAr. This is due to the signal sources being widely spaced, reducing the requirement for DCA continuity. Overall, the errors of all arrays increase with the rise of $|c_1|$, and when the signal sources are far apart, the arrays exhibit more accurate resolution.

D. $2q$ th-Order NRA and MRA

To demonstrate the feasibility of the proposed framework for high-order cumulants, we consider the case of $q = 2$, which involves a non-redundant array (PNRA $2q$) and two types of minimum-redundant arrays (PMRAr $2q$ and PMRAg $2q$) using fourth-order cumulants. Figs. 15 and 16 illustrate their array element locations and $2q$ th-order difference co-arrays ($q = 2$), respectively.

The effectiveness of our proposed framework in $2q$ th-order array design is evident from Fig. 16, where it can be observed that the $2q$ th-order difference co-arrays meet the design requirements of non-redundant and minimum-redundant arrays. This demonstrates the success and validity of our proposed framework in $2q$ th-order array design.

To compare with the latest work, we consider the fractal geometry method in [45]. It utilizes a small array as a generator and employs fractal geometry to expand this generator into a large array, which can inherit certain properties of the generator. The fractal geometry approach allows for the rapid and convenient generation of large arrays. However, it should be noted that the redundancy property can not be inherited. To show the above point, Table II analyzes the result of sparse array design using the fractal geometry method with $[0, 1, 3]$ as the generator array. we denote the resulting fourth-order large

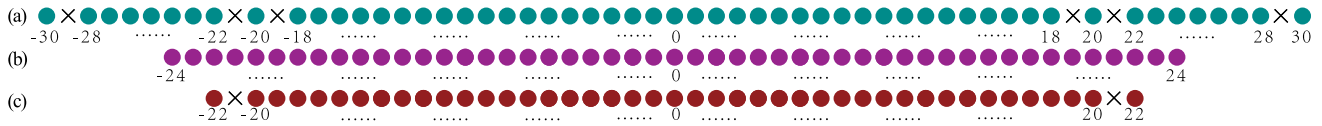


Fig. 16. $2q$ -level difference co-arrays of different types of 4-element $2q$ -level non-redundant and minimum-redundant linear sparse arrays ($q = 2$). (a) Proposed $2q$ -level non-redundant array. (b) Proposed $2q$ -level minimum-redundant array under restricted case. (c) Proposed $2q$ -level minimum-redundant array under general case.

TABLE II
DIFFERENTIAL ARRAY ANALYSIS OF 4TH-O-FRACTAL IN [45]

Generator Array	0,1,3
4th-O-Fractal	0,1,3,7,8,10,21,22,24,73,171,367,416,514,1053,1102,1200
Number of elements in 4-level DCA	18905
Number of redundant elements in 4 level DCA (except 0)	15142
Number of holes in DCA	1164

array as 4th-O-Fractal. It is observed that while the generator array is a minimum-redundant and non-redundant array, the difference co-array of expanded 4th-O-Fractal array contains 15142 redundant array elements and 1164 holes. Consequently, the generated high-order array is neither non-redundant nor a minimum redundant array, indicating it does not satisfy the redundancy requirements for the given number of array elements. In contrast, the proposed method can achieve optimal design for non-redundant or minimum-redundant arrays, although it may require longer computation time when designing large arrays.

VII. CONCLUSION

This paper concerns the concepts of non-redundant arrays and minimum-redundant arrays, thereby identifying key conditions that must be met in array design. Subsequently, we proposed a novel framework for sparse array design using integer programming. By formulating non-redundant and minimum-redundant array designs as integer linear programming problems, we have enabled flexible array design with specific constraints. Our approach accommodates redundancy requirements and practical limitations simultaneously, and even extending to higher-order moment scenarios.

To demonstrate the effectiveness of the proposed framework, extensive simulations were performed and the results showed that arrays meeting specific requirements can be generated using the framework. Furthermore, DOA estimation performance evaluation shows clear advantages compared to other existing methods. The proposed framework allows to design arrays with desirable properties and to achieve reliable DOA estimation accuracy.

REFERENCES

- [1] H. L. V. Trees, *Optimum array processing: Part IV of detection, estimation, and modulation theory*. Hoboken, NJ, USA: Wiley, 2004.
- [2] H. Dai, Z. Zhang, S. Gong, C. Xing, and J. An, "Training optimization for subarray based IRS-assisted MIMO communications," *IEEE Internet Things J.*, vol. 9, no. 4, pp. 2890–2905, Feb. 2022.
- [3] R. T. Hoctor and S. A. Kassam, "The unifying role of the co-array in aperture synthesis for coherent and incoherent imaging," *Proc. IEEE*, vol. 78, no. 4, pp. 735–752, Apr. 1990.
- [4] L. R. Haupt, *Antenna arrays: A computational approach*. New York, NY, USA: Wiley, 2010.
- [5] M. Huan, J. Liang, Y. Wu, Y. Li, and W. Liu, "SASA: Super-resolution and ambiguity-free sparse array geometry optimization with aperture size constraints for MIMO radar," *IEEE Trans. Antennas Propag.*, vol. 71, no. 6, pp. 4941–4954, Jun. 2023.
- [6] M. Guo, Y. D. Zhang, and T. Chen, "DOA estimation using compressed sparse array," *IEEE Trans. Signal Process.*, vol. 66, no. 15, pp. 4133–4146, Aug. 2018.
- [7] D. H. Johnson and D. E. Dudgeon, *Array Signal Processing: Concepts and Techniques*. Englewood Cliffs, NJ, USA: Prentice Hall, 1992.
- [8] E. Vertatschitsch and S. Haykin, "Nonredundant arrays," *Proc. IEEE*, vol. 74, no. 1, pp. 217–217, Jan. 1986.
- [9] A. Ahmed and Y. D. Zhang, "Generalized non-redundant sparse array designs," *IEEE Trans. Signal Process.*, vol. 69, pp. 4580–4594, 2021.
- [10] A. Moffet, "Minimum-redundancy linear arrays," *IEEE Trans. Antennas Propag.*, vol. AP-16, no. 2, pp. 172–175, Mar. 1968.
- [11] P. Pal and P. P. Vaidyanathan, "Nested arrays: A novel approach to array processing with enhanced degrees of freedom," *IEEE Trans. Signal Process.*, vol. 58, no. 8, pp. 4167–4181, Aug. 2010.
- [12] M. Yang, L. Sun, X. Yuan, and B. Chen, "Improved nested array with hole-free DCA and more degrees of freedom," *Electron. Lett.*, vol. 52, no. 25, pp. 2068–2070, Dec. 2016.
- [13] P. Zhao, G. Hu, Z. Qu, and L. Wang, "Enhanced nested array configuration with hole-free co-array and increasing degrees of freedom for DOA estimation," *IEEE Commun. Lett.*, vol. 23, no. 12, pp. 2224–2228, Dec. 2019.
- [14] P. P. Vaidyanathan and P. Pal, "Sparse sensing with co-prime samplers and arrays," *IEEE Trans. Signal Process.*, vol. 59, no. 2, pp. 573–586, Feb. 2011.
- [15] P. Pal and P. P. Vaidyanathan, "Coprime sampling and the MUSIC algorithm," in *Proc. IEEE Digit. Signal Process. Signal Process. Educ. Meeting*, 2011, pp. 289–294.
- [16] X. Wang and X. Wang, "Hole identification and filling in k-times extended co-prime arrays for highly efficient DOA estimation," *IEEE Trans. Signal Process.*, vol. 67, no. 10, pp. 2693–2706, May 2019.
- [17] W. Zheng, X. Zhang, Y. Wang, J. Shen, and B. Champagne, "Padded coprime arrays for improved DOA estimation: Exploiting hole representation and filling strategies," *IEEE Trans. Signal Process.*, vol. 68, pp. 4597–4611, 2020.
- [18] P. Ma, J. Li, F. Xu, and X. Zhang, "Hole-free coprime array for DOA estimation: Augmented uniform co-array," *IEEE Signal Process. Lett.*, vol. 28, pp. 36–40, 2021.
- [19] W. Zheng, X. Zhang, J. Li, and J. Shi, "Extensions of co-prime array for improved DOA estimation with hole filling strategy," *IEEE Sensors*, vol. 21, no. 5, pp. 6724–6732, Mar. 2021.
- [20] J. Shi, F. Wen, Y. Liu, Z. Liu, and P. Hu, "Enhanced and generalized coprime array for direction of arrival estimation," *IEEE Trans. Aerosp. Electron. Syst.*, vol. 59, no. 2, pp. 1327–1339, Apr. 2023.
- [21] T. Svantesson, "Modeling and estimation of mutual coupling in a uniform linear array of dipoles," in *Proc. IEEE Int. Conf. Acoust., Speech, Signal Process.*, pp. 2961–2964, 1999.
- [22] C.-L. Liu and P. P. Vaidyanathan, "Super nested arrays: Linear sparse arrays with reduced mutual coupling—Part I: Fundamentals," *IEEE Trans. Signal Process.*, vol. 64, no. 15, pp. 3997–4012, Aug. 2016.
- [23] C.-L. Liu and P. P. Vaidyanathan, "Super nested arrays: Linear sparse arrays with reduced mutual coupling—Part II: High-order extensions," *IEEE Trans. Signal Process.*, vol. 64, no. 16, pp. 4203–4217, Aug. 2016.
- [24] J. Liu, Y. Zhang, Y. Lu, S. Ren, and S. Cao, "Augmented nested arrays with enhanced DOF and reduced mutual coupling," *IEEE Trans. Signal Process.*, vol. 65, no. 21, pp. 5549–5563, Nov. 2017.

- [25] A. Raza, W. Liu, and Q. Shen, "Thinned coprime array for second-order difference co-array generation with reduced mutual coupling," *IEEE Trans. Signal Process.*, vol. 67, no. 8, pp. 2052–2065, Apr. 2019.
- [26] Z. Zheng, W.-Q. Wang, Y. Kong, and Y. D. Zhang, "MISC array: A new sparse array design achieving increased degrees of freedom and reduced mutual coupling effect," *IEEE Trans. Signal Process.*, vol. 67, no. 7, pp. 1728–1741, Apr. 2019.
- [27] W. Shi, Y. Li, and R. C. de Lamare, "Novel sparse array design based on the maximum inter-element spacing criterion," *IEEE Trans. Signal Process. Lett.*, vol. 29, pp. 1754–1758, 2022.
- [28] X. Sheng, D. Lu, Y. Li, and R. C. de Lamare, "Enhanced MISC-based sparse array with high uDOFs and low mutual coupling," *IEEE Trans. Circuits Syst. II: Exp. Briefs*, vol. 71, no. 2, pp. 972–976, Feb. 2024.
- [29] D. H. Werner, R. L. Haupt, and P. L. Werner, "Fractal antenna engineering: The theory and design of fractal antenna arrays," *IEEE Trans. Antennas Propag. Mag.*, vol. 41, no. 5, pp. 37–58, Oct. 1999.
- [30] D. H. Werner and S. Ganguly, "An overview of fractal antenna engineering research," *IEEE Trans. Antennas Propag. Mag.*, vol. 45, no. 1, pp. 38–57, Feb. 2003.
- [31] C. Puente-Baliarda and R. Pous, "Fractal design of multiband and low sidelobe arrays," *IEEE Trans. Antennas Propag.*, vol. 44, no. 5, pp. 730–739, May 1996.
- [32] R. Cohen and Y. C. Eldar, "Sparse array design via fractal geometries," *IEEE Trans. Signal Process.*, vol. 68, pp. 4797–4812, Aug. 2020.
- [33] R. Cohen and Y. C. Eldar, "Sparse fractal array design with increased degrees of freedom," *Proc. IEEE Int. Conf. Acoust., Speech, Signal Process.*, 2019, pp. 4195–4199.
- [34] K. J. Falconer, *Fractal Geometry: Mathematical Foundations and Applications*. Hoboken, NJ, USA: Wiley, 2014.
- [35] C.-L. Liu and P. P. Vaidyanathan, "Robustness of difference coarrays of sparse arrays to sensor failures—Part I: A theory motivated by coarray MUSIC," *IEEE Trans. Signal Process.*, vol. 67, no. 12, pp. 3213–3226, Jun. 2019.
- [36] C.-L. Liu and P. P. Vaidyanathan, "Robustness of difference coarrays of sparse arrays to sensor failures—Part II: Array geometries," *IEEE Trans. Signal Process.*, vol. 67, no. 12, pp. 3227–3242, Jun. 2019.
- [37] C.-L. Liu and P. P. Vaidyanathan, "Novel algorithms for analyzing the robustness of difference coarrays to sensor failures," *Signal Process.*, vol. 171, no. 107517, Jun. 2020, Art. no. 107517.
- [38] C.-L. Liu and P. P. Vaidyanathan, "Optimizing minimum redundancy arrays for robustness," in *Proc. IEEE 52nd Asilomar Conf. Signals, Syst., Comput.*, 2018, pp. 79–83.
- [39] C.-L. Liu and P. P. Vaidyanathan, "Composite singer arrays with hole-free coarrays and enhanced robustness," in *Proc. IEEE Int. Conf. Acoust., Speech, Signal Process.*, 2019, pp. 4120–4124.
- [40] D. Zhu, S. Wang, and G. Li, "Multiple-fold redundancy arrays with robust difference coarrays: Fundamental and analytical design method," *IEEE Trans. Antennas Propag.*, vol. 69, no. 9, pp. 5570–5584, Sep. 2021.
- [41] P. Chevalier, A. Ferreol, and L. Albera, "High-resolution direction finding from higher order statistics: The $2q$ -MUSIC algorithm," *IEEE Trans. Signal Process.*, vol. 54, no. 8, pp. 2986–2997, Aug. 2006.
- [42] G. Birot, L. Albera, and P. Chevalier, "Sequential high-resolution direction finding from higher order statistics," *IEEE Trans. Signal Process.*, vol. 58, no. 8, pp. 4144–4155, Aug. 2010.
- [43] P. Pal and P. P. Vaidyanathan, "Multiple level nested array: An efficient geometry for $2q$ th order cumulant based array processing," *IEEE Trans. Signal Process.*, vol. 60, no. 3, pp. 1253–1269, Mar. 2012.
- [44] Q. Shen, W. Liu, W. Cui, S. Wu, and P. Pal, "Simplified and enhanced multiple level nested arrays exploiting high-order difference coarrays," *IEEE Trans. Signal Process.*, vol. 67, no. 13, pp. 3502–3515, Jul. 2019.
- [45] Z. Yang, Q. Shen, W. Liu, Y. C. Eldar, and W. Cui, "High-order cumulants based sparse array design via fractal geometries—Part I: Structures and DOFs," *IEEE Trans. Signal Process.*, vol. 71, pp. 327–342, 2023.
- [46] Z. Yang, Q. Shen, W. Liu, Y. C. Eldar, and W. Cui, "High-order cumulants based sparse array design via fractal geometries—Part II: Robustness and mutual coupling," *IEEE Trans. Signal Process.*, vol. 71, pp. 343–357, 2023.
- [47] *Gurobi Optimizer Reference Manual*. Gurobi Optimization, Briarwood, TX, USA, 2023.
- [48] *IBM ILOG CPLEX optimization Studio CPLEX Users Manual*, IBM, Raleigh, NC, USA, 2018.
- [49] C. Zhou, Y. Gu, X. Fan, Z. Shi, G. Mao, and Y. D. Zhang, "Direction-of-arrival estimation for coprime array via virtual array interpolation," *IEEE Trans. Signal Process.*, vol. 66, no. 22, pp. 5956–5971, Nov. 2018.



Yangjingzhi Zhuang (Student Member, IEEE) was born in Sichuan, China, in 1997. She received the B.S. degree in electronic information engineering in 2019 from the University of Electronic Science and Technology of China (UESTC), where she is currently working toward the Ph.D. degree in information and communication engineering. Currently, she is a Visiting Student with the University of Pisa, Italy. Her research interests include array signal processing, irregular array optimization, and integer programming.



Xuejing Zhang (Member, IEEE) was born in Hebei, China. He received the B.S. degree in electrical engineering from Huaqiao University, Xiamen, China, in 2011, the M.S. degree in signal and information processing from Xidian University, Xi'an, China, in 2014, and the Ph.D. degree in signal and information processing from the University of Electronic Science and Technology of China, Chengdu, China, in 2019. From 2017 to 2019, he was a Visiting Student with the University of Delaware, Newark, DE, USA. Currently, he is an Associate Professor with the School of Information and Communication Engineering, University of Electronic Science and Technology of China. His research interests include array signal processing and integer programming, with applications to radar and communications. He was awarded the Young Scientists Award for Excellence in Scientific Research by the International Union of Radio Science (URSI) in 2020. He received the Prize for Excellent Doctor Degree Dissertation of the Chinese Institute of Electronics in 2020.



Zishu He (Senior Member, IEEE) was born in Sichuan, China, in 1962. He received the B.S., M.S., and Ph.D. degrees in signal and information processing from the University of Electronic Science and Technology of China (UESTC), in 1984, 1988, and 2000, respectively. Currently, he is a Professor in signal and information processing with the School of Information and Communication Engineering, UESTC. His research interests include array signal processing, digital beam forming, the theory of multiple-input multiple-output (MIMO) communication and MIMO radar, adaptive signal processing, and interference cancellation.



Maria Sabrina Greco (Fellow, IEEE) is with the Department of Information Engineering, University of Pisa, where she has been a Full Professor since 2017. Her general interests are in the areas of statistical signal processing, estimation, and detection theory. In particular, her research interests include clutter models, coherent and incoherent detection in non-Gaussian clutter, CFAR techniques, radar waveform diversity, bistatic/multistatic active and passive radars, cognitive radars, and integration of sensing and communications. She has co-authored

many book chapters and more than 250 journal and conference papers. She was the co-recipient of the 2001 and 2012 IEEE Aerospace and Electronic Systems Society's Barry Carlton Awards for Best Paper published in the IEEE TRANSACTIONS ON AEROSPACE AND ELECTRONIC SYSTEMS (T-AES), the co-recipient of the 2019 EURASIP *Journal on Advances in Signal Processing* (JASP) Best Paper Award, and the co-recipient of the 2019 H. Mimno Award for the Best Paper published in the *IEEE Aerospace and Electronic Systems Magazine*. She received the 2008 Fred Nathanson Young Engineer of the Year Award for contributions to signal processing, estimation, and detection theory, and the IEEE Aerospace and Electronic Systems Society (AESS) Board of Governors Exceptional Service Award for "Exemplary Service and Dedication and Professionalism, as EiC of the *IEEE Aerospace and Electronic Systems Magazine*". She has been the General Chair, Technical Program Chair, and Organizing Committee Member of many international conferences over the last ten years. She has also been the Lead Guest Editor of many special issues on Radar Signal Processing. She is currently the Editor-in-Chief of the *EURASIP Journal on Advances in Signal Processing*. She has been a member of the IEEE Signal Processing Society (SPS) Board of Governors (2015–2017), the Chair of the IEEE AESS Radar Panel (2015–2016), the SPS Distinguished Lecturer for 2014–2015, the AESS Distinguished Lecturer, the AESS Vice President of Publications (2018–2020), the Editor-in-Chief of the *IEEE Aerospace and Electronic Systems Magazine*, and the IEEE SPS Director-at-Large for Region 8 (2021–2022). She is now the President of AESS (2024–2025).



Fulvio Gini (Fellow, IEEE) received the Doctor Engineer (*cum laude*) and the Research Doctor degrees in electronic engineering from the University of Pisa, Italy, in 1990 and 1995, respectively. In 1993, he joined the Department of Ingegneria dell'Informazione of the University of Pisa, where he became an Associate Professor in 2000 and he is a Full Professor since 2006. Prof. Gini is the Deputy Head of the Department since 2016. From 1996 to 1997, he was a Visiting Researcher with the Department of Electrical Engineering, University

of Virginia, Charlottesville. He is an Associate Editor for the IEEE TRANSACTIONS ON AEROSPACE AND ELECTRONIC SYSTEMS since 2007 and for the Elsevier *Signal Processing Journal* since 2006. He has been an AE for the IEEE TRANSACTIONS ON SIGNAL PROCESSING (2000–2006) and is a Senior AE of the same TRANSACTION since 2016. He was a member of the EURASIP JASP Editorial Board. He was co-founder and 1st Co-Editor-in-Chief of the *Hindawi International Journal on Navigation and Observation* (2007–2011). He was an Area Editor for the Special issues of the *IEEE Signal Processing Magazine* (2012–14). He was co-recipient of the 2001 and 2012 IEEE AES Society's Barry Carlton Award for Best Paper published in the IEEE TRANSACTIONS ON AES. He was recipient of the 2003 IEE Achievement Award for outstanding contribution in signal processing and of the 2003 IEEE AES Society Nathanson Award to the Young Engineer of the Year. He is a member of the Radar System Panel (2008–present) and of the Board of Governors (BoG) (2017–2019) of the IEEE Aerospace and Electronic Systems Society (AESS). He is a member of the IEEE SPS Awards Board (2016–2018). He has been a Member of the *Signal Processing Theory and Methods* (SPTM) Technical Committee (TC) of the IEEE SIGNAL PROCESSING SOCIETY AND OF THE SENSOR ARRAY AND MULTICHANNEL (SAM) TC for many years. He is a member of the Board of Directors (BoD) of the EURASIP Society, the Award Chair (2006–2012) and the EURASIP President (2013–2016). He is the General Co-Chair of the 2020 IEEE Radar conference to be held in Florence in 2020. He was the Technical Co-Chair of the 2006 EURASIP Signal and Image Processing Conference (EUSIPCO 2006), Florence (Italy), of the 2008 Radar Conference, Rome (Italy), and of the 2015 IEEE CAMSAP workshop, Cancun (Mexico). He was the General Co-Chair of the 2nd Workshop on Cognitive Information Processing (CIP2010), of the 2014 IEEE International Conference on Acoustics, Speech and Signal Processing (ICASSP 2014), held in Florence (Italy), and of the 2nd, 3rd and 4th editions of the workshop on Compressive Sensing in Radar (CoSeRa). Prof. Gini was the Section Editor for the "Radar Signal Processing" section, vol. 3 of the Academic Press Library in Signal Processing, S. Theodoridis and R. Chellappa editors, Elsevier Ltd., 2013. Prof. Gini's career spans more than 25 years, during which he has made numerous foundational contributions to radar systems and radar signal processing. His technical contributions are captured in 171 journal articles, 191 conference papers, 13 book chapters, and 2 Italian patents. h-index: 55. Citations: 11 400 (Google Scholar).